

A notable bounded probability distribution for environmental and lifetime data

Hassan S. Bakouch¹, Tassaddaq Hussain², Christophe Chesneau³ and Tamás Jónás⁴

¹ *Department of Mathematics, Faculty of Science, Tanta University, Tanta, Egypt,*

Email: hassan.bakouch@science.tanta.edu.eg

² *Mirpur University of Science and Technology (MUST), 10250 Mirpur (AJK), Pakistan,*

Email: tafkho2000@gmail.com

³ *Université de Caen, LMNO, Campus II, Science 3, 14032, Caen, France,*

Email: christophe.chesneau@unicaen.fr

⁴ *Faculty of Economics, Eötvös Loránd University, Budapest, Hungary,*

Email: jonas@gtk.elte.hu

Abstract

In this article, we introduce a notable bounded distribution based on a modification of the epsilon function which creates an upper bound on the domain of the distribution. Further, a key feature of the distribution links the readers with the asymptotic connections with the famous Lindley distribution, which is a weighted variant of the exponential distribution and also a mixture of exponential and gamma distributions. In some ways, the proposed distribution provides a flexible solution to the modeling of bounded characteristics that can be almost well-fitted by the Lindley distribution if the domain is restricted. Moreover, we have also explored its application, particularly with reference to lifetime and environmental points of view, and found that the proposed model exhibits a better fit among the competing models. Further, from the annual rainfall analysis, the proposed model exhibits a realistic return period of the rainfall.

Keywords: Epsilon distribution, Lindley distribution, Practical analysis, Applications, Hydrological measure.

AMS Subject Classification: 60E05, 62E15, 62F10.

1 Introduction

While observing real life phenomena, one usually comes across finite range of changes. Such finite changes generally give rise to bounded domain distributions. Among these bounded distributions, an upper bound is very helpful in analysing the annual stream flow and annual rainfall data (see Phien and Ajirajah (1984)). The most common bounded domain distributions are the uniform, power, Bates, arcsin, Kumaraswamy, Topp-Leone, beta, triangular, raised cosine, and Von Mises distributions. As an alternative to these distributions, Dombi *et al.* (2018) recently introduced the epsilon distribution (EpD). Mathematically, it is based on the epsilon function defined by

$$\varepsilon_{\lambda,d}(x) = \begin{cases} \left(\frac{d+x}{d-x}\right)^{\lambda\frac{d}{2}}, & \text{if } -d < x < d, \\ 0, & \text{otherwise,} \end{cases}$$

30 where $\lambda \in \mathbb{R}$, $\lambda \neq 0$, $d > 0$. This function is derived from the first-order epsilon differential equation
 31 and has the property of satisfying the following exponential limit property: For any $x \in (-d, +d)$,
 32 if $d \rightarrow \infty$, then $\varepsilon_{\lambda,d}(x) \rightarrow e^{\lambda x}$. Hence, a continuous random variable X is said to have an epsilon
 33 distribution with the parameters $\lambda > 0$ and $d > 0$ if its cumulative distribution function (CDF) is
 34 given by

$$35 \quad F_{\lambda,d}^*(x) = \begin{cases} 0, & \text{if } x \leq 0, \\ 1 - \varepsilon_{-\lambda,d}(x), & \text{if } 0 < x < d, \\ 1, & \text{if } x \geq d. \end{cases}$$

37 As a result, the epsilon distribution is a bounded domain distribution with two parameters and
 38 satisfies the following limiting property: $\lim_{d \rightarrow +\infty} F_{\lambda,d}^*(x) = F_{\lambda}^*(x)$, where $F_{\lambda}^*(x)$ is the CDF of
 39 the exponential distribution with parameter λ . Among the applications, according to Dombi *et al.*
 40 (2018), the epsilon distribution can be used to describe the mortality and useful life cycle in the
 41 sense of reliability management under the assumption of a typical bathtub-shaped failure rate.

42 In this paper, we propose a notable two-parameter distribution also based on the epsilon func-
 43 tion but connected to the famous Lindley distribution, instead of the exponential distribution. The
 44 Lindley distribution has a plural interest. First, it was created by Lindley (1958, 1965). It was
 45 first coined to express the distinction between fiducial and posterior distributions, and it has been
 46 widely used in mathematical theory and practice in recent years. Let us recall that the cumulative
 47 density function (CDF) of the Lindley distribution with parameter $\lambda > 0$ is given by

$$48 \quad F_{\lambda}^o(x) = \begin{cases} 0, & \text{if } x \leq 0, \\ 1 - \left(1 + \frac{\lambda x}{1 + \lambda}\right) e^{-\lambda x}, & \text{if } x > 0. \end{cases}$$

50 The Lindley distribution has been used to analyze large amounts of data, especially in the context
 51 of stress resistance and reliability modeling. There is a substantial literature on the Lindley distri-
 52 bution. Let us mention the Lindley distribution's dominance over the exponential distribution of
 53 banking customers' waiting times until service, as highlighted by Ghitany *et al.* (2008), the Lind-
 54 ley distribution's applications in lifetime data in the context of competing risks, as presented by
 55 Mazucheli and Achcar (2011), and a comparison study of the adequacy of exponential and Lindley
 56 distributions, as presented by Shanker *et al.* (2015) and Shanker and Mishra (2013), among others.

57 By capturing the idea of the epsilon distribution and adapting it to reach the Lindley distribution
 58 as a limit, we motivate the use of the following function:

$$59 \quad F_{\lambda,d}(x) = \begin{cases} 0, & \text{if } x \leq 0, \\ 1 - \left(1 + \frac{\lambda}{1 + \lambda} \frac{dx}{d - x}\right) \varepsilon_{-\lambda,d}(x), & \text{if } 0 < x < d, \\ 1, & \text{if } x \geq d, \end{cases} \quad (1)$$

61 where $\lambda > 0$ and $d > 0$. The distribution defined by $F_{\lambda,d}(x)$ is called the epsilon-Lindley distribution
 62 (EpLD). Then, one can prove that it is a CDF, which satisfies $\lim_{d \rightarrow +\infty} F_{\lambda,d}(x) = F_{\lambda}^o(x)$; the Lindley
 63 distribution is a limit case of the EpLD, which is a rare property for a bounded support distribution.
 64 Furthermore, the related functions, such as the probability density function (PDF) and hazard rate
 65 function (HRF) are very flexible in their behaviour, as shown later. More precisely, by using a
 66 graphical analysis, the PDF adopt various shapes, like skewed to the right with J-shapes as well as
 67 an upside down U-shape. In all these cases, we observe a positive skewness and leptokurtic nature of
 68 the curve, which clearly indicates that it is designed to model the heavy-tailed phenomenon. Such

69 phenomena are generally common in reliability applications, queuing theory and environmental
70 aspects. In this regard, we focus on the environmental aspect and also lifetime direction. Our
71 application section will help the reader to reach a decision to forecast the next generation's future
72 in a better way. Environmental data analysis is based on the most efficient bounded models.
73 One can mention the three parameter log normal distribution, generalized extreme value type II
74 distribution, generalized extreme value type III distribution, three parameter gamma distribution,
75 and three parameter log-Pearson distribution, among others. The non-closed form of the CDF in
76 these popular hydrological models is a fundamental flaw, whereas the suggested model is based on
77 only two parameters and has a closed form of its basic functions, including its CDF, which makes
78 the determination of the return period considerably easier.

79 Further, the HRF adopts various shapes, from bathtub to increasing failure rate with a left
80 skewed J-shape. This functional flexibility is a real plus for the EpLD from the modeling viewpoint.
81 On the mathematical plan, the EpLD is a weighted version of the EpD. This weighted version not
82 only models ascertainment biases but also a linear combination of probability distributions. We thus
83 develop the statistical features offered by the EpLD through diverse aspects, including theoretical
84 and practical facts. The practical lines interested in fitting, modeling and analysis of lifetime and
85 environmental data are outlined by the proposed model. Further, from the annual rainfall analysis,
86 we found a realistic return period of the rainfall by the proposed model.

87 The organization of the paper is as follows. Section 2 presents some other functions of interest
88 in the EpLD like moments and parameter estimation. Section 3 covers the application area of
89 the proposed model. Section 4 deals with conclusion and closing comments about the proposed
90 distribution.

91 2 Some Related Functions, Properties with Estimation

92 2.1 Related Functions

93 We now illustrate the shape behavior of the main functions of the EpLD. First, let us focus on the
94 CDF as defined in Equation (1). Figure 1 presents some graphs of this CDF for several values of
95 the parameters.

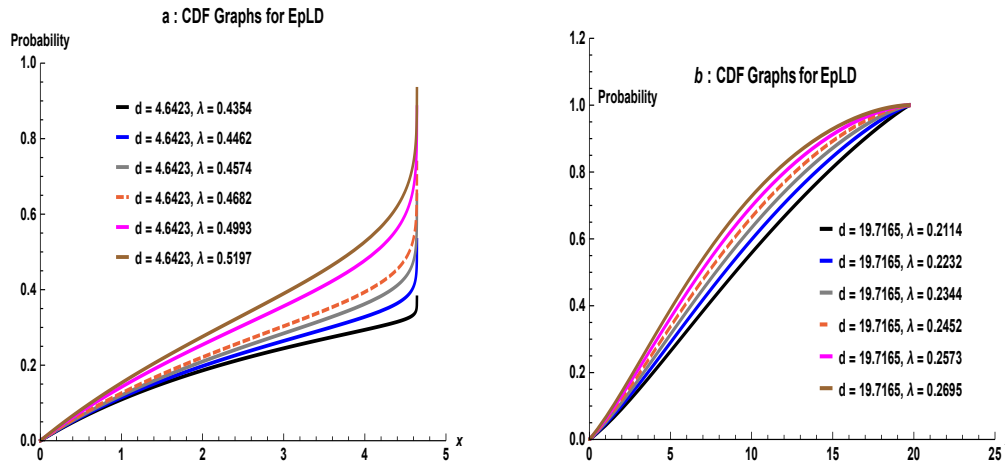


Figure 1: Graphs of CDF of the EpLD

96 Figure 1 depicts that for smaller values of both d and λ , the convergence of CDF to 1 is very

97 slow compared to that for larger d and λ values.

98 Let us now focus on the related PDF. The PDF of the EpLD is expressed as

$$99 \quad f_{\lambda,d}(x) = \begin{cases} \frac{\lambda d^2}{(1+\lambda)(d^2-x^2)} \left[1 + \lambda - \frac{d+x-\lambda dx}{d-x} \right] \varepsilon_{-\lambda,d}(x), & \text{if } 0 < x < d, \\ 0, & \text{otherwise.} \end{cases} \quad (2)$$

100

101 Figure 2 presents some graphs of this PDF for several parameter values.

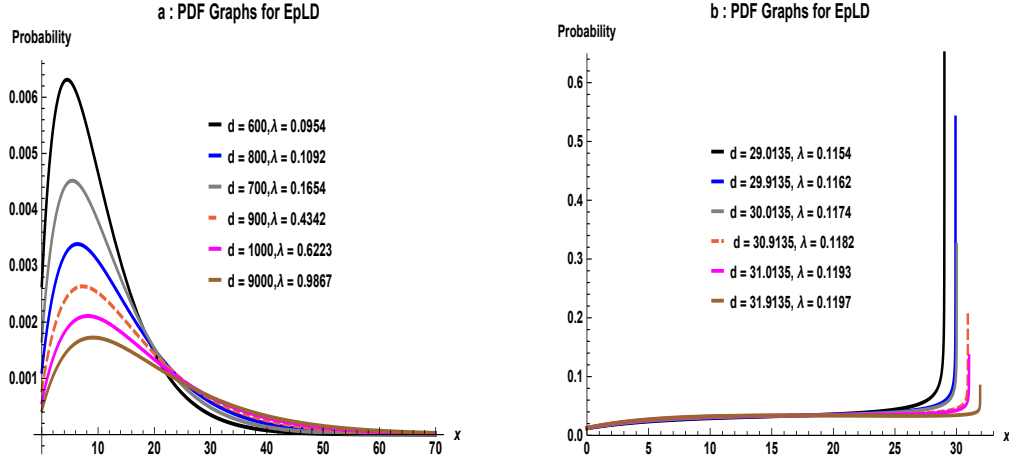


Figure 2: Graphs of PDF of the EpLD; unimodal shapes skewed to the right and J shapes

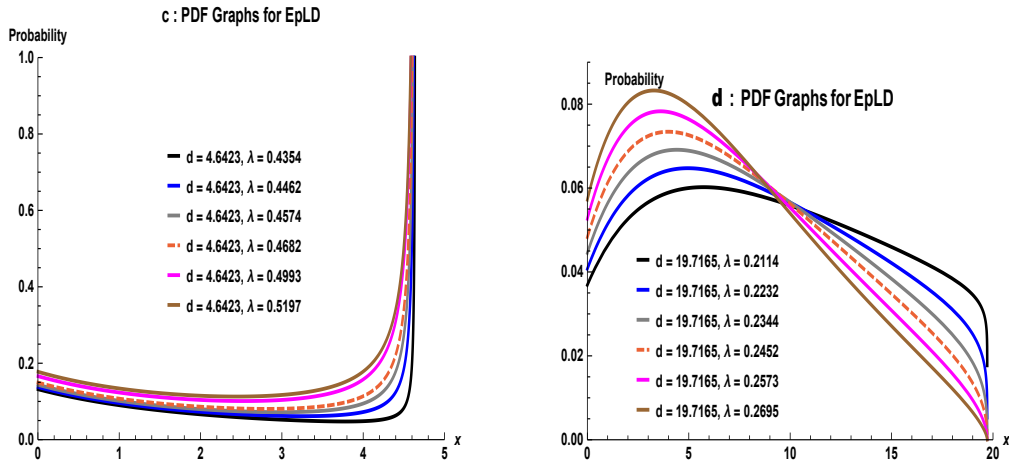


Figure 3: Graphs of PDF of the EpLD; U-J shapes and upside down U-shapes

102 From Figures 2 and 3, we see that the PDF of the EpLD also adopts various shapes, like
 103 unimodal shapes skewed to the right, various J-shapes, as well as an upside down U-shapes. In par-
 104 ticular, Figure 2-b indicates that when the rate parameter λ decreases, it increases the probability
 105 of events whatever the boundary value of x , i.e., d is. Thus, the PDF of the EpLD distribution is
 106 extremely flexible, and, as developed in the introductory section, motivates the use of the EpLD
 107 for various modelling purposes, including the heavy-tailed phenomenon.

108 In addition to its practical ability, the PDF of the EpLD has interesting mathematical decom-
 109 positions. Indeed, one can view $f_{\lambda,d}(x)$ as follows:

- 110 • It is a weighted version of the PDF of the EpD, because it can be written as $f_{\lambda,d}(x) =$
 111 $w_{\lambda,d}(x)f_{\lambda,d}^*(x)$, where

$$112 \quad w_{\lambda,d}(x) = 1 - \frac{d+x-\lambda dx}{(1+\lambda)(d-x)}$$

113 and $f_{\lambda,d}^*(x)$ refers to the PDF of the epsilon distribution.
 114

- 115 • Assuming that $\lambda > 2/d$, by noticing that

$$116 \quad \frac{d+x-\lambda dx}{(1+\lambda)(d-x)} = \frac{1}{1+\lambda} \left[\frac{\lambda}{4}(d-x) + \left(1 - \frac{\lambda}{4}(d+x)\right) \frac{d+x}{d-x} \right],$$

117 we can also write $f_{\lambda,d}(x)$ as a linear combination of PDFs and length biased PDFs of the
 118 EpD as

$$119 \quad f_{\lambda,d}(x) = \left(1 - \frac{\lambda}{4(1+\lambda)}(d-x)\right) f_{\lambda,d}^*(x) - \frac{\lambda d}{(1+\lambda)(\lambda d-2)} \left(1 - \frac{\lambda}{4}(d+x)\right) f_{\lambda-2/d,d}^*(x) \\
 120 \quad = \left(1 - \frac{\lambda d}{4(1+\lambda)}\right) f_{\lambda,d}^*(x) - \frac{\lambda d}{(1+\lambda)(\lambda d-2)} \left(1 - \frac{\lambda d}{4}\right) f_{\lambda-2/d,d}^*(x) \\
 121 \quad + \frac{\lambda}{4(1+\lambda)} x f_{\lambda,d}^*(x) + \frac{\lambda^2 d}{4(1+\lambda)(\lambda d-2)} x f_{\lambda-2/d,d}^*(x). \quad (3)$$

123 This expansion is useful to determine several probabilistic quantities related to the EpLD.

124 As a major reliability function of the EpLD, the HRF is specified as

$$125 \quad h_{\lambda,d}(x) = \begin{cases} \frac{\lambda d^2}{(1+\lambda)(d^2-x^2)} \left[1 + \lambda - \frac{d+x-\lambda dx}{d-x}\right] \left(1 + \frac{\lambda}{1+\lambda} \frac{dx}{d-x}\right)^{-1}, & \text{if } 0 < x < d, \\ 0, & \text{otherwise.} \end{cases}$$

127 Figure 4 provides some graphs of this HRF for selected values of the parameters.

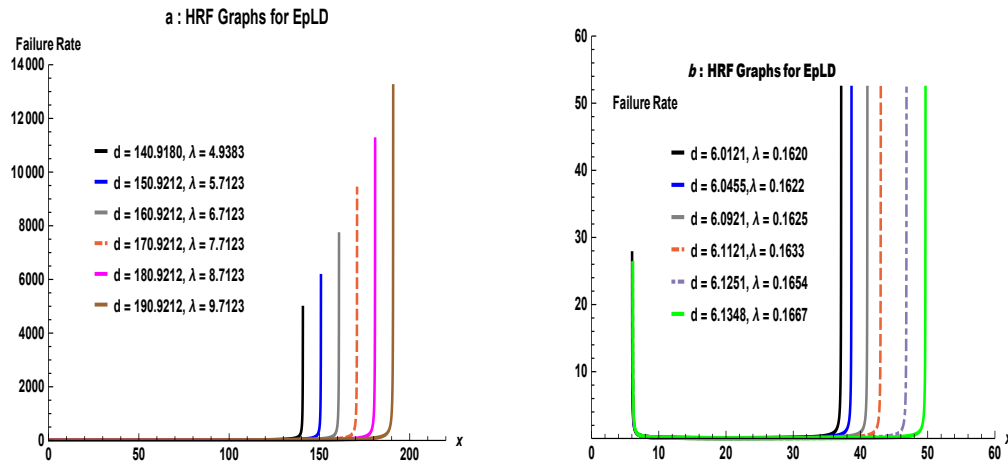


Figure 4: Graphs of HRF of the EpLD

128 The graphs in Figure 4 clearly portray the HRF behaviour like increasing and bathtub shape
 129 in an impressive way.

130 We end this part by discussing the quantile analysis of the EpLD. As we know, in traditional
 131 probability and statistics as well as in stochastic analysis, the quantile function (QF) deals with a
 132 valuable way of describing a static or vigorous distribution, as a result, knowing how to use this
 133 function indicates certain advantages not available straight from the CDF or PDF. For example,
 134 the simplest way of simulating any non-uniform random variable is by applying its QF to uniform
 135 deviates. Similarly, from an environmental point of view, these functions usually help environmental
 136 scientists to calculate the return period and return level of any distribution.

137 In view of above, the QF of the EpLD, denoted by $Q_{\lambda,d}(u)$ with $u \in (0, 1)$, is the solution of
 138 the following non-linear equation:

$$139 \left(1 + \frac{\lambda}{1 + \lambda} \frac{dQ_{\lambda,d}(u)}{d - Q_{\lambda,d}(u)} \right) \varepsilon_{-\lambda,d}[Q_{\lambda,d}(u)] = 1 - u.$$

140 To evaluate $Q_{\lambda,d}(u)$ at given u and parameters, it is clear that mathematical software is required.

141 2.2 Moments

142 In mathematics and statistics, the word moments of a function are reckonable procedures associated
 143 to the shape of the function's graph. If the function represents density or mass function, then the
 144 first moment represent the center of the mass or expected value, and the second moment is the
 145 rotational inertia or the variance. So, the moments about the origin of the EpLD can be determined
 146 by using the expansion in Equation (3). For a random variable $Y_{\lambda,d}$ following the epsilon distribution
 147 with parameters λ and d and a random variable X following the EpLD, the r -th moment of X can
 148 be obtained as

$$149 \mu'_r = E(X^r) = \left(1 - \frac{\lambda d}{4(1 + \lambda)} \right) E(Y_{\lambda,d}^r) - \frac{\lambda d}{(1 + \lambda)(\lambda d - 2)} \left(1 - \frac{\lambda d}{4} \right) E(Y_{\lambda-2/d,d}^r) \\ 150 + \frac{\lambda}{4(1 + \lambda)} E(Y_{\lambda,d}^{r+1}) + \frac{\lambda^2 d}{4(1 + \lambda)(\lambda d - 2)} E(Y_{\lambda-2/d,d}^{r+1}).$$

152 The the r -th and $(r + 1)$ -th moments of $Y_{\lambda,d}$ are well established, see Okorie and Nadarajah (2019).
 153 In a similar way, we can express the incomplete moments of X in terms of incomplete moments of
 154 $Y_{\lambda,d}$. Thus, the mean and variance of X can be obtained.

155 Similarly, the ratio of third mean moment to the square of second mean moment are the skewness
 156 and the ratio fourth moment about mean to second moment about mean is the kurtosis. Moreover,
 157 these moments are not only determine the shape of a function but also help to characterize the
 158 probability function. From these moments we are now able to interpret the shape and kurtosis
 159 behaviour of the EpLD. In this regard, Figure 5 portrays that the proposed model can exhibit
 160 versatile shapes ranging from negative to positive behaviour. In addition, the distribution can also
 161 exhibit the leptokurtic, mesokurtic and platykurtic behaviour which are evident in Figure 5.

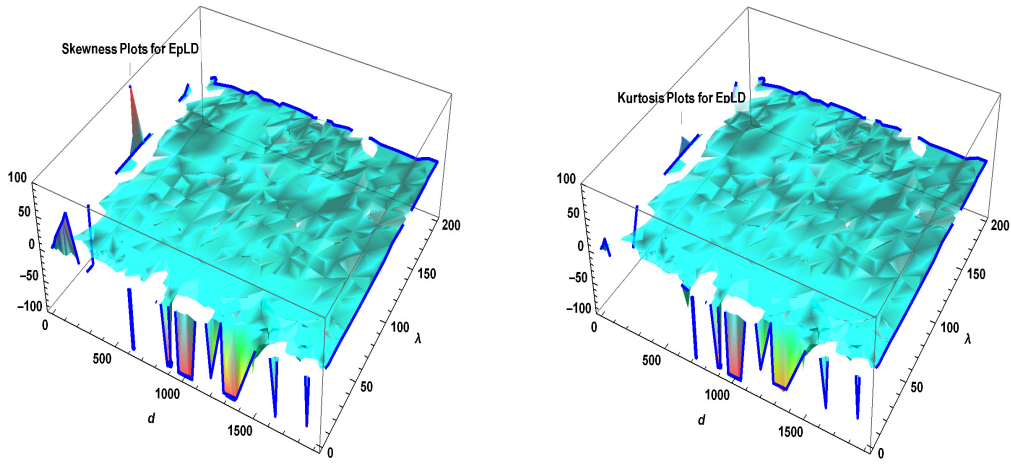


Figure 5: Graphs of skewness and kurtosis of the EpLD

162 2.3 Parameters estimation

163 Due to the importance of statistical inference, here we adopt the maximum likelihood method
 164 (MLEs) for estimation purpose which is the most commonly employed method. MLEs are designed
 165 to follow the regularity conditions which are usually helpful for constructing the confidence inter-
 166 vals and the test statistics. For these estimators, the large sample theory yields straightforward
 167 approximations that works well in finite samples. In order to achieve better approximation dis-
 168 tributions, statisticians frequently strive to estimate quantities, such as the distribution of a test
 169 statistic that depends on the sample size. The resulting MLE approximation in distribution theory
 170 can be handled analytically or numerically with ease. Only complete samples are used to calculate
 171 the maximum likelihood estimates (MLEs) of the EpLD parameters. In this regard, let x_1, \dots, x_n
 172 be a realization of a random sample of size n from the EpLD given by Equation (2). Then the
 173 log-likelihood function of the EpLD is given by

$$\begin{aligned}
 174 \quad \ell(\lambda, d) &= 2n \log d + n \log \lambda - n \log(1 + \lambda) - \left(1 + \frac{d\lambda}{2}\right) \sum_{i=1}^n \log \left(\frac{d + x_i}{d - x_i}\right) \\
 175 \quad &+ \sum_{i=1}^n \log [d\lambda + x_i((d - 1)\lambda - 2)] - 3 \sum_{i=1}^n \log(d - x_i). \quad (4) \\
 176
 \end{aligned}$$

177 The log-likelihood can be maximized either directly by using the Mathematica [12.0] or by solving
 178 the nonlinear likelihood equations obtained by differentiating Equation (4).

$$\begin{aligned}
 179 \quad \frac{\partial \ell(\lambda, d)}{\partial \lambda} &= \frac{n}{\lambda} - \frac{n}{1 + \lambda} - \frac{d}{2} \sum_{i=1}^n \log \left(\frac{d + x_i}{d - x_i}\right) + \sum_{i=1}^n \frac{d + (d - 1)x_i}{d\lambda + ((d - 1)\lambda - 2)x_i}. \\
 180
 \end{aligned}$$

181 The MLE of the parameter λ is obtained by solving the nonlinear system $\partial \ell(\lambda, d)/\partial \lambda = 0$. Since
 182 this equation cannot be solved analytically, so we prefer to use statistical packages like Mathe-
 183 matica [12.0]. For this purposes we used Global MLEs of the proposed model which take Lindley
 184 distribution MLEs as seed value. However, we have observed that we cannot obtain the estimate
 185 of d from Equation (4). In order to obtain MLE of d we adopted the methodology as, since d is
 186 free from x and it is the upper limit in the domain of x , so we suppose that $x_{(1)}, x_{(2)}, \dots, x_{(n)}$,

187 denotes the ordered sample corresponding to x_1, x_2, \dots, x_n this implies that the MLE for d as
 188 $\hat{d} = \max(x_1, x_2, \dots, x_n) + v$, where $v > 0$ denotes an arbitrary constant. However, when we start to
 189 estimate a parameter, d of a distribution using the sample, we undertake that all the elements in the
 190 sample are in the domain of the random variable. This is because the sample should be comprised
 191 of independent observations on the random variable in demand. Since the value of parameter d
 192 determines the domain of attraction of the random variable that has a EpLD, in the estimation,
 193 it is a necessity that d is greater than the maximal element in the sample. So we are looking for
 194 the robust value of \hat{d} which will probably be established under the condition that \hat{d} is greater than
 195 the largest element in the sample. Moreover, the convergence of proposed model's MLEs depends
 196 upon the huge value of \hat{d} , i.e., $\hat{d} \rightarrow \infty$ which follows the standard epsilon distribution theory, for
 197 more details, the reader is referred to Dombi *et al.* (2018), Dombi *et al.* (2019), Dombi and Jónás
 198 (2020) and Dombi and Jónás (2021).

199 3 Model compatibility and its Application to Real-World Data

200 In this section, we will concentrate on the modelling process's model selection and model validation.
 201 However, model selection is a challenging task and the prime of a suitable model and it is produced
 202 with the use of well-considered judgement based on whatever information is available. It is essential
 203 that the chosen model should be malleably sufficient to model the confronted data amply, while
 204 considering the settlement between simplicity of evaluation and the intricacy of the model.

205 Moreover, outstanding devotion must be waged to modeling behavior for large and small values
 206 of the variable of interest. In this regard, the modelling process includes validating the model,
 207 which includes various goodness-of-fit tests and graphical procedures. These statistical techniques
 208 for assessing hypothesised models are known as goodness-of-fit tests. An unsatisfactory fit, either
 209 analytical or graphical, may occur for the following reasons: i) The model is incorrectly specified.
 210 ii) The model specification is correct, but unfortunately carries a huge bias. In general, validation
 211 demands additional data, other information, and further testing as well as careful assessment of
 212 the fallouts.

213 3.1 Goodness-of-Fit Tests

214 As in such tests, researchers usually make a null hypothesis, H_0 : The given data comes from a
 215 CDF with a specified form. For this purpose, we have considered four tests. The first test is
 216 the most famous χ^2 test (Chi Square), due to Karl Pearson. It includes grouping observed data
 217 into intervals and may be used to assess the fit of data to any specified distribution (continuous
 218 or discrete). When using this test, a sample of size n is assumed, with each observation falling
 219 into one of k potential classifications. The observed and expected frequencies in the interval i are
 220 denoted by o_i and e_i , respectively. The test statistic is

$$221 \chi^2 = \sum_{i=1}^k \frac{(o_i - e_i)^2}{e_i}.$$

222
 223 However, this test has the advantages of being easy to apply and being applicable even when
 224 parameters are unknown (see Murthy, *et al.* (2004)). In addition, this test is considered a powerful
 225 test that is why it is not of much use in small or sometimes even modest size samples (see Murthy,
 226 *et al.* (2004)). The next three tests are based on the empirical cumulative distribution function
 227 (ECDF) and hence are often referred to as ECDF tests.

228 **3.2 Kolmogorov-Smirnov (KS) Test**

229 The Kolmogorov-Smirnov (KS) test is grounded on the ECDF. Given n ordered observations
 230 Z_1, Z_2, \dots, Z_k , then the ECDF is defined as $E_k = m_i/k$ where m_i is the number of points less
 231 than Z_i and the Z_i are ordered from smallest to largest value. At the value of each ordered data
 232 point, this step function rises by $1/k$. The greatest distance between the hypothesised CDF and
 233 ECDF is the test statistic KS. The mathematical expression of KS is given by

234
$$\text{KS} = \max_{1 \leq i \leq k} \left\{ \frac{i}{k} - z_i, z_i - \frac{i-1}{k} \right\},$$

235

236 where z_i is the theoretical cumulative distribution of the distribution being tested. Other goodness-
 237 of-fit tests, like the Anderson-Darling test and the Cramér Von-Mises test, are alternatives of the
 238 KS test. As these modified tests are usually measured to be more powerful than the conventional
 239 KS test, many analysts prefer them.

240 **3.3 Anderson-Darling (AD_0^*) Test**

241 The Anderson-Darling (AD_0^*) test is an alternative of the KS test and usually attaches more weight
 242 to the tails than the KS test. Its test statistic is

243
$$A_0^* = \left(\frac{2.25}{k^2} + \frac{0.75}{k} + 1 \right) \left\{ -k - \frac{1}{k} \sum_{i=1}^k (2i-1) \log(z_i(1-z_{k-i+1})) \right\}.$$

244

245 **3.4 Cramér-von Mises (CVM_0^*) Test**

246 CVM_0^* test is also a modification of the KS test. Which is usually considered to be more powerful
 247 than the original KS test. The CVM_0^* test is expressed as

248
$$W_0^* = \sum_{i=1}^k \left(z_i - \frac{2i-1}{2k} \right)^2 + \frac{1}{12k}.$$

249

250 A relative comparison of the selection of these tests indicates that: i) The ECDF tests are more
 251 powerful than the χ^2 test. ii) The KS test is the most well-known ECDF test, but it is often
 252 much less powerful than the other ECDF tests (AD_0^* and CVM_0^* tests) (see Murthy, *et al.* (2004)).
 253 Moreover, we have also applied information criteria for model selection purposes, such as Akaike
 254 information criterion (AIC), Bayesian information criterion (BIC), corrected Akaike information
 255 criterion (AICc), Hannan-Quinn information criterion (HQIC) and consistent Akaike information
 256 criterion (CAIC). The following are the definitions of AIC, AICc, HQIC, and CAIC:

257
$$\text{AIC} = 2\hat{\hbar} - 2l, \quad \text{AICc} = \text{AIC} + \frac{2\hat{\hbar}(\hat{\hbar} + 1)}{n - \hat{\hbar} - 1}, \quad \text{BIC} = \hat{\hbar} \log(n) - 2l,$$

258

259

260
$$\text{HQIC} = -2l + \hat{\hbar} \log(\log(n)), \quad \text{CAIC} = -2l + \frac{2\hat{\hbar}n}{n - \hat{\hbar} - 1},$$

261

262 where l denotes the estimate of the maximum log-likelihood function, $\hat{\hbar}$ is the number of parameters
 263 to be estimated and n is the number of data.

264 Along with these model selection procedures, we have also used the Kullback-Leibler information
 265 criterion philosophy and applied the Vuong test proposed by Vuong (1989).

266 3.5 Vuong Test

267 It is a closeness test based on the likelihood-ratio-based test for model selection using the Kullback-
 268 Leibler information criterion philosophy. This test may be used for non-nested models, and it
 269 generally compares the null hypothesis that the two competing models are equally near to the
 270 actual data against the alternative that one model performs better. Further discussion about
 271 Vuong statistics can be found in Hussain *et al.* (2019).

272 3.6 Competing Models

273 We compare the proposed model with the following well known models: epsilon probability distri-
 274 bution (EpD) (see Dombi *et al.* (2018)), two parameter Lindley (TPLD) distribution (see Shanker
 275 *et al.* (2015)), A quasi Lindley distribution (QLD) (see Shanker and Mishra (2013)), Lindley distri-
 276 bution (LD) (see Lindley (1958)) and exponential distribution (ED). For the sake of transparency,
 277 these competitors are defined by the following PDFs:

- 278 • for the EpD:

$$279 \quad f_{\lambda,d}^{EpD}(x) = \frac{\lambda d^2}{d^2 - x^2} \varepsilon_{-\lambda,d}(x), \quad 0 < x < d,$$

280
 281 and $f_{\lambda,d}^{EpD}(x) = 0$ for $x \notin [0, d]$, with $d > 0$,

- 282 • for the TPLD:

$$283 \quad f_{\lambda,d}^{TPLD}(x) = \frac{\lambda^2(1+dx)}{d+\lambda} e^{-\lambda x}, \quad x > 0,$$

284
 285 and $f_{\lambda,d}^{TPLD}(x) = 0$ for $x \leq 0$, with $\lambda > 0$ and $d > -1$,

- 286 • for the QLD:

$$287 \quad f_{\lambda,d}^{QLD}(x) = \frac{\lambda(d+\lambda x)}{d+1} e^{-\lambda x}, \quad x > 0,$$

288
 289 and $f_{\lambda,d}^{QLD}(x) = 0$ with $\lambda > 0$ and $d > -1$,

- 290 • for the LD:

$$291 \quad f_{\lambda}^{LD}(x) = \frac{\lambda^2(1+x)}{1+\lambda} e^{-\lambda x}, \quad x > 0,$$

292
 293 and $f_{\lambda}^{LD}(x) = 0$ for $x \leq 0$, with $\lambda > 0$,

- 294 • for the ED:

$$295 \quad f_{\lambda}^{ED}(x) = \lambda e^{-\lambda x}, \quad x > 0,$$

296
 297 and $f_{\lambda}^{ED}(x) = 0$, with $\lambda > 0$.

298 We consider four different real-world data sets.

299 **3.7 Lifetime Data Sets**

300 **Data sets I and II.** The first and second data sets are taken from Walpole *et al.* (2012) and
 301 Andrews and Herzberg (1985), respectively. The first data represent the length of life in years,
 302 measured to the nearest tenth of 30 similar fuel pumps, while the second data represent the life of
 303 fatigue fracture of Kevlar 373 epoxy that is subjected to constant pressure at the 90 stress level
 304 until all have failed. The measurements of the first data set are 2.0, 3.0, 0.3, 3.3, 1.3, 0.4, 0.2, 6.0,
 305 5.5, 6.5, 0.2, 2.3, 1.5, 4.0, 5.9, 1.8, 4.7, 0.7, 4.5, 0.3, 1.5, 0.5, 2.5, 5.0, 1.0, 6.0, 5.6, 6.0, 1.2, 0.2. The
 306 second data set measurements are given as: 0.0251, 0.0886, 0.0891, 0.2501, 0.3113, 0.3451, 0.4763,
 307 0.5650, 0.5671, 0.6566, 0.6748, 0.6751, 0.6753, 0.7696, 0.8375, 0.8391, 0.8425, 0.8645, 0.8851, 0.9113,
 308 0.9120, 0.9836, 1.0483, 1.0596, 1.0773, 1.1733, 1.2570, 1.2766, 1.2985, 1.3211, 1.3503, 1.3551, 1.4595,
 309 1.4880, 1.5728, 1.5733, 1.7083, 1.7263, 1.7460, 1.7630, 1.7746, 1.8275, 1.8375, 1.8503, 1.8808, 1.8878,
 310 1.8881, 1.9316, 1.9558, 2.0048, 2.0408, 2.0903, 2.1093, 2.1330, 2.2100, 2.2460, 2.2878, 2.3203, 2.3470,
 311 2.3513, 2.4951, 2.5260, 2.9911, 3.0256, 3.2678, 3.4045, 3.4846, 3.7433, 3.7455, 3.9143, 4.8073, 5.4005,
 312 5.4435, 5.5295, 6.5541, 9.0960. In this regard, we have compiled the descriptive statistics which
 313 are listed in Table 1 and the total time on test (TTT) plot introduced by Aarset (1987), which is
 314 portrayed in Figure 6 for Data sets I and II. In particular, the TTT plot indicates the empirical
 315 HRF and estimated behaviour of the HRF of the EpLD are very close to each other as compared
 316 to the competing models.

Data set	Sample size	Mean	Median	Standard deviation	Skewness	Kurtosis	$\frac{Skewness}{Kurtosis}$
I	30	2.7967	2.1500	2.2273	0.3412	1.5689	0.2175
II	76	1.9592	1.5335	1.6753	1.9796	8.1608	0.2426

Table 1: Descriptive statistics for Data sets I and II.

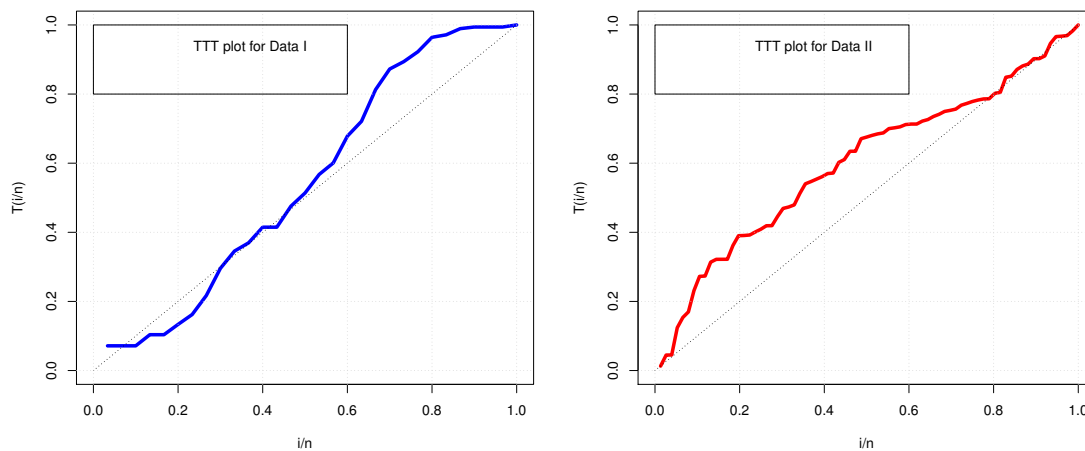


Figure 6: Estimated TTT plots of Data sets I and II

Data set	Sample size	Mean	Median	Standard deviation	Skewness	Kurtosis	$\frac{Skewness}{Kurtosis}$
I	30	2.7802	2.2285	2.2505	1.1766	4.2477	0.2769
II	76	1.9589	1.5739	1.7362	1.4309	5.4976	0.2602

Table 2: Theoretical statistics from the EpLD

317 3.7.1 Discussion and Analysis of Lifetime Data Sets

318 Tables 1 and 2 reveal that theoretical and observed descriptive statistics show a remarkable closeness
319 to each other and it seems that both data sets are being simulated by the proposed model.

Distribution	$\hat{\lambda}$	\hat{d}	CVM ₀ *	AD ₀ *	KS	$\chi^2(df)$	p-value
EpLD	0.5839	1219.9011	0.5059	0.0728	0.1408	1.0760(2)	0.5839
EpD	0.3575	6.31×10^6	0.7569	0.1189	0.1358	1.6246(2)	0.4438
TPLD	0.3575	-1.92×10^{-26}	0.7569	0.1189	0.1358	1.6246(2)	0.4438
QLD	0.5123	1.3097	0.5512	0.0809	0.1341	1.0990(2)	0.5772
LD	0.5834	...	0.5061	0.0729	0.1409	1.0767(2)	0.5831
ED	0.3576	...	0.7569	0.1189	0.1358	1.6246(2)	0.4438

Table 3: MLEs and goodness-of-fit statistics for Data set I

320 Note that as the parameter d specifies the support of of the PDF of the EpLD in Equation
321 (2), i.e., it is positive only if $x \in (0, d)$. This means that the value of parameter d must meet
322 the requirement $d > \max_{i=1,2,\dots,n}(x_i)$, see Dombi *et al.* (2019). That is why we observed that \hat{d}
323 is large for any data set, as shown in the related tables. From the TTT-plot for Data set I, we
324 can see that the curve has three characteristic phases: (1) a first convex phase, where the failure
325 rate is decreasing; (2) a second quasi linear phase with a constant failure rate; (3) and a third
326 concave phase, where the failure rate is increasing. That is, the TTT-plot for Data set I portrays
327 a bathtub-shaped like failure rate curve. Noting the TTT-plot for Data set II, we can conclude
328 that it exhibits an increasing failure rate phenomenon of the empirical failure rate function. Hence,
329 both of the above data sets are efficiently modelled by the proposed model. Since d is large, EpLD
330 is almost identical to LD, and so they have almost the same goodness values. Such a suitability
331 of the proposed model is reflected in Tables 3 and 4, where the EpLD yields a smallest value of
332 the goodness of fit statistics along with highest p-vlaue for χ^2 statistics. In addition, we have also
333 accessed the performance of the model with respect to LD via the log-likelihood ratio test, which
334 is usually applicable for nested models, which clearly indicates that.

Distribution	$\hat{\lambda}$	\hat{d}	CVM_0^*	AD_0^*	KS	$\chi^2(df)$	p-value
EpLD	0.7948	99910.0267	1.4902	0.2667	0.1156	6.8497(6)	0.3349
EpD	0.5104	40763.1154	3.2134	0.5746	0.1663	13.4562(6)	0.0363
TPLD	0.5104	8.29×10^{-10}	3.0187	0.5746	0.1663	13.4562(6)	0.0363
QLD	0.9542	0.1499	0.6003	0.1016	0.1025	9.3621(8)	0.3126
LD	0.7947	...	1.4902	0.2668	0.1156	6.8496(6)	0.3348
ED	0.5104	...	3.0188	0.5746	0.1663	13.4562(6)	0.0363

Table 4: MLEs and goodness-of-fit statistics for Data set II

335 However, Tables 5 and 6 portray that QLD and LD yield minimum values of information
336 criterion, which some seem to be a penalty of over parametrization, particularly with reference to
337 the LD model. Previously we pointed out that the LD distribution may be viewed as an asymptotic
338 EpLD distribution, i.e., if $d \rightarrow \infty$, then the EpLD distribution is identical to the LD distribution.
339 We can observe a practical implication of this finding in the tables from Table 3-6. Namely, when
340 a data set can be modelled well by the LD distribution, then it can also be modelled well by an
341 EpLD distribution with a sufficiently large value of parameter d , and vice versa. Certainly, in such
342 a case, the estimates of the λ parameters and the corresponding goodness-of-fit statistics are very
343 close.

Distribution	$-l$	AIC	AICC	BIC	HQIC	CAIC
EpLD	60.7645	125.529	125.973	128.331	123.977	125.973
EpD	60.8525	125.705	126.149	128.507	124.153	126.149
TPLD	60.8529	125.706	126.15	128.508	124.154	126.15
QLD	60.4864	124.973	125.417	127.775	123.421	125.417
LD	60.7668	123.534	123.676	124.935	123.982	123.676
ED	60.8528	123.706	123.848	125.107	124.154	123.848

Table 5: Estimate of the maximum log-likelihood and information criteria for Data set I

Distribution	$-l$	AIC	AICC	BIC	HQIC	CAIC
EpLD	123.674	251.348	251.512	256.009	250.279	251.512
EpD	127.114	258.228	258.392	262.889	257.159	258.392
TPLD	127.114	258.228	258.392	262.889	257.159	258.392
QLD	121.65	247.3	247.464	251.961	246.231	247.464
LD	123.675	249.35	249.404	251.681	250.281	249.404
ED	127.114	258.228	258.392	262.889	257.159	258.392

Table 6: Estimate of the maximum log-likelihood and information criteria for Data set II

344 Furthermore, Table 7 also pleads for the suitability of the proposed model. But Vuong statistics
345 show that QLD and LD are strong competitors for the proposed model.

Models	Data set I	Suitability	Data set II	Suitability
EpLD- EpD	2.7872	EpLD	32.5790	EpLD
EpLD-TPD	2.7872	EpLD	32.5804	EpLD
EpLD-QLD	-0.9287	Indecisive	-15.3623	QLD
EpLD-LD	1513.008	EpLD	-1321291	LD
EpLD-ED	2.7872	EpLD	32.5790	EpLD

Table 7: Vuong test statistics for Data sets I and II

346 Furthermore, an analysis of the histogram’s form revealed that we can observe from Figure 7
 347 that the proposed model matches the data in a better way than competing models.

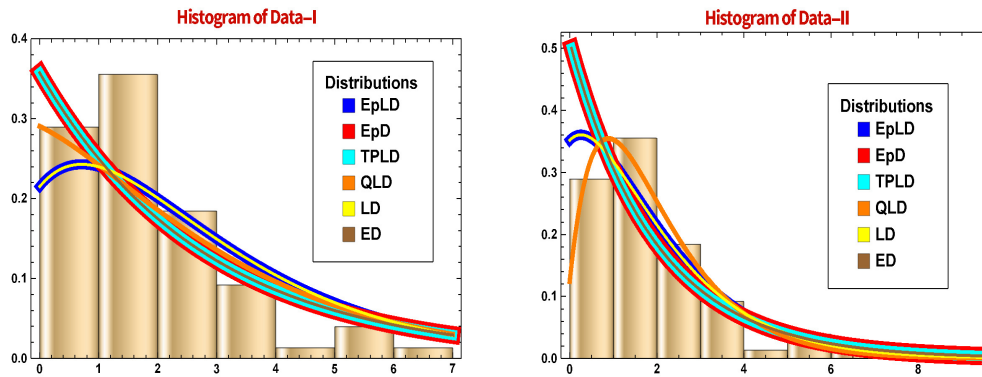


Figure 7: Data sets I and II fit via histograms

348 3.8 Environmental Data Sets

349 **Data sets III and IV.** The third and fourth data sets are the total amount of rain fall in mm of
 350 Pakistani cities Lasbella and Bunji which covers a period of 30 years (1981 to 2010) with 30 values
 351 of annual rain fall in each set. They were reported by Hussain *et al.* (2019). The third data set
 352 measurements are as follows: 138.11818, 89.5, 246.5, 142.6, 143.5, 47.4, 105.7, 182.6, 153.7, 119.9,
 353 56.5, 272.8, 99.9, 426.1, 205.6, 169.8, 308.3, 80.5, 104.0, 37.7, 223.0, 9.2, 474.6, 25.3, 209.6, 182.5,
 354 196.2, 254.9, 103.6, 117.6. The fourth data set contains the following rainfall measurements: 248.8,
 355 82.2, 102.2, 217.9, 113.2, 248.2, 244.1, 122.2, 144.9, 63.2, 62.8, 139, 228.7, 216.4, 144.8, 252.6, 144.8,
 356 157.2, 168.5, 139.1, 74.3, 154.6, 339.4, 154.1, 156.3, 200.7, 97.5, 96.3, 155.2, 298.8, respectively. The
 357 descriptive statistics of these data sets and corresponding theoretical statistics from the EpLD are
 358 presented in the Tables 8 and 9, respectively. Box-plots of the data are given in Figure 8.

Data set	Sample size	Mean	Median	Standard deviation	Skewness	Kurtosis	$\frac{Skewness}{Kurtosis}$
III	30	164.241	143.05	108.163	1.1201	4.2629	0.2627
IV	30	165.6	154.35	70.3731	0.5800	2.7073	0.2142

Table 8: Descriptive statistics for Data sets III and IV

Data set	Sample size	Mean	Median	Standard deviation	Skewness	Kurtosis	$\frac{Skewness}{Kurtosis}$
III	30	163.952	138.302	114.483	1.0747	4.0723	0.2639
IV	30	176.0789	160.9816	102.6899	0.5248	2.5549	0.2054

Table 9: Theoretical statistics from the EpLD

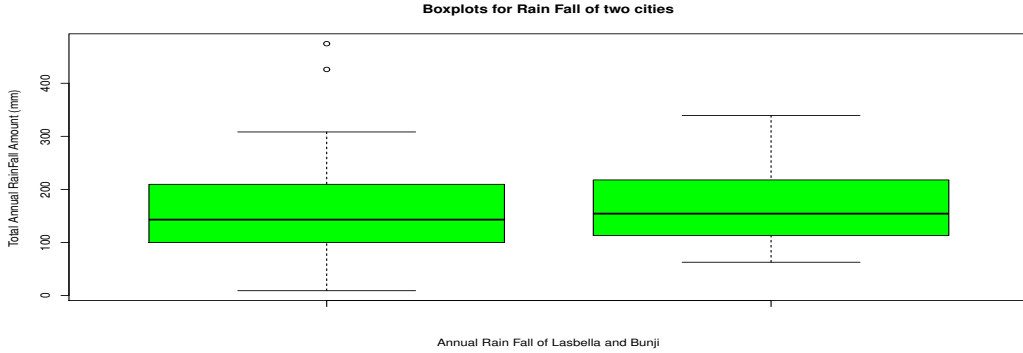


Figure 8: Box-plots for Data sets III and IV

359 In order to analyse the environmental data, we have also checked some features of the envi-
360 ronmental data, namely homogeneity, independence and stationarity. For this purpose, we applied
361 the Mann-Whitney (M-W) test for testing homogeneity and stationarity, and the Mann-Kendall
362 (M-K) test for trend detection. In this regard, we have observed that both data sets accept the hy-
363 potheses of homogeneity and stationarity at a 5 percent level of significance with Z-scores of 0.3568
364 and -0.2777, respectively. Similarly, the hypothesis of independence and identically distributed
365 distribution is accepted at a 5 percent level of significance with Z-scores of 0.4817 and -0.6943,
366 respectively. For details of these tests, readers are referred to Haktanir *et al.* (2013).

367 3.8.1 Analysis and Discussion of Environmental Data

368 From Table 8 and Figure 8 as well as Table 9, it is obvious that the empirical and theoretical aspects
369 of the data sets in the presence of outliers in Data set III are in close agreement and indicate that
370 the model can effectively be used if the data are positively skewed and leptokurtic in nature, which
371 are the obvious characteristics of environmental data. Such findings are further consolidated by
372 viewing Tables 10 and 11 which portray that the EpLD exhibits minimum values of goodness of fit
373 statistics.

Distribution	$\hat{\lambda}$	\hat{d}	CVM_0^*	AD_0^*	KS	$\chi^2(df)$	p-value
EpLD	0.0122	8329.81	0.0472	0.2778	0.1117	0.2294(2)	0.8916
EpD	0.0041	9.29×10^6	1.8655	0.3667	0.2417	3.6401(2)	0.1620
TPLD	0.00411	0.0000	0.3667	1.8655	0.2417	3.6401(2)	0.1620
QLD	0.0121	0.0159	0.0479	0.2796	0.1122	0.2350(2)	0.8891
LD	0.0121	...	0.0473	0.2779	0.1121	0.2296(2)	0.8915
ED	0.0061	...	0.3549	1.8494	0.2224	3.3397(2)	0.1883

Table 10: MLEs and goodness-of-fit statistics for Data set III

Distribution	$\hat{\lambda}$	\hat{d}	CVM_0^*	AD_0^*	KS	$\chi^2(df)$	p-value
EpLD	0.0123	498.906	0.2002	1.3785	0.1650	2.5612(1)	0.1096
EpD	0.0060	9.25×10^7	0.8954	4.6593	0.3156	10.7892(1)	0.0010
TPLD	0.0060	6.56×10^{-13}	0.8954	4.6594	0.3156	10.3156(1)	0.0013
QLD	0.0121	-4.12×10^{-27}	0.3099	1.8943	0.1898	2.7965(1)	0.0945
LD	0.0120	...	0.3164	1.9301	0.1904	2.8808(1)	0.0896
ED	0.0060	...	0.8954	4.6593	0.3156	10.7892(1)	0.0010

Table 11: MLEs and goodness-of-fit statistics for data set IV

374 Tables 10 and 11 indicate that ECDF test statistics for goodness-of-fit tests are low, which
375 ensures that the EpLD is a good competitor to QLD and LD.

376 However, likelihood aspects and information criterion values also favour the proposed model,
377 which can be visualized in Tables 12 and 13, respectively.

Distribution	$-l$	AIC	AICC	BIC	HQIC	CAIC
EpLD	179.123	362.247	362.691	365.049	360.695	362.691
EpD	183.04	370.08	370.524	372.882	368.528	370.524
TPLD	183.04	370.08	370.524	372.882	368.528	370.524
QLD	179.125	362.251	362.695	365.053	360.699	362.695
LD	179.13	360.26	360.403	361.661	360.708	360.403
ED	183.04	368.08	368.223	369.481	368.528	368.223

Table 12: Estimate of the maximum log-likelihood and information criteria for Data set III

Distribution	$-l$	AIC	AICC	BIC	HQIC	CAIC
EpLD	173.351	350.703	351.147	353.505	349.151	351.147
EpD	183.287	370.575	371.019	373.377	369.023	371.019
TPLD	183.287	370.575	371.019	373.377	369.023	371.019
QLD	174.435	352.869	353.314	355.672	351.318	353.314
LD	174.576	351.152	351.294	352.553	351.6	351.294
ED	183.287	368.575	368.717	369.976	369.023	368.717

Table 13: Estimate of the maximum log-likelihood and information criteria for Data set IV

378 Furthermore, the shape of our proposed model, as shown in Figure 9, matches the data in a
379 better way compared to competing models.

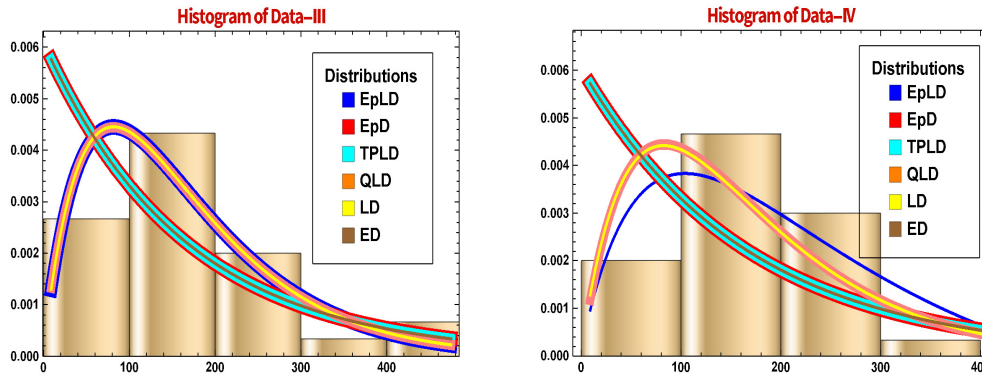


Figure 9: Data sets III and IV fit via histograms

380 Furthermore, Vuong statistics as depicted in Table 14 also show the capability of the proposed
381 model.

Models	Data set III	Suitability	Data set IV	Suitability
EpLD- EpD	19.4212	EpLD	56.0414	EpLD
EpLD-TPD	19.4213	EpLD	56.0412	EpLD
EpLD-QLD	1954.888	EpLD	8.5923	EpLD
EpLD-LD	-39411	LD	9.8278	EpLD
EpLD-ED	16.7418	EpLD	56.0414	EpLD

Table 14: Vuong test statistics for Data sets III and IV

382 3.8.2 Hydrological Parameters

383 The annual series is very common in frequency analysis for two reasons. The earliest is its accessi-
384 bility, as most data are managed in such a way that the annual series is commonly available. The
385 other one is that there is a simple hypothetical basis for deducing the frequency of annual series
386 data beyond the range of observation (see World Meteorological Organization (2009)). Moreover,
387 we observed that both series are valid and approved by the M-W and M-K tests, as shown in the
388 earlier section.

389 Therefore, it can be settled that, according to the consequences of relevant tests, both the
 390 annual rainfall series documented at Lasbella (Pakistan) and Bounji (Pakistan) are homogeneous,
 391 independent, non-periodic and trend-free. Hence, classical frequency analyses are applied to all of
 392 the annual rainfall series. From the above mentioned analysis, we can conjecture that the EpLD is
 393 a suitable model for the above mentioned data sets, so we have decided to portray its return period
 394 for those interested in environmental data, which is being studied in the coming subsection.

395 3.8.3 Return Period

396 The average number of years in which an event is predicted to be equalled or exceeded only once is
 397 the return period \mathfrak{T} of a particular level. The return period is the reciprocal of the probability of
 398 exceeding the threshold in a particular year (see World Meteorological Organization (2009)). The
 399 link between the annual return time and the exceedance probability may be stated as follows
 400 if the yearly exceedance probability is designated $1/\mathfrak{T}$. Since the probability of exceedance is
 401 $P(X > x_{\mathfrak{T}}) = 1/\mathfrak{T}$, this implies a return level with a return period of $\mathfrak{T} = 1/p$ is a high threshold
 402 $x_{\mathfrak{T}}$ whose probability of exceedance is p .

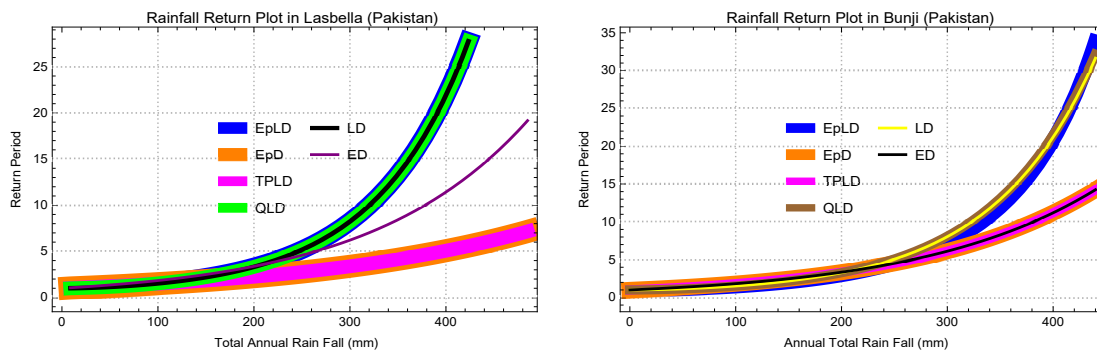


Figure 10: Return periods of the competing models for Data sets III and IV

403 In this regard, we have studied that the EpLD yields a realistic return period which can be
 404 visualized from Figure 10.

405 4 Conclusion

406 In this article, we proposed a notable bounded distribution under the name epsilon Lindley dis-
 407 tribution (EpLD). This new distribution provides a flexible solution to the problem of modeling
 408 bounded characteristics. This feature of EpLD is based on the finding that this distribution can be
 409 treated as a bounded alternative of the well-known Lindley distribution. Here, we estimated the
 410 parameters of EpLD using the maximum likelihood method. Next, we studied the applications of
 411 the proposed distribution both in lifetime and environmental data modeling. Based on the empir-
 412 ical results, we could conclude that the proposed methodology works quite well. In particular, for
 413 the annual rainfall data set, the EpLD yields a realistic return period when compared with other
 414 competing models.

415 Author contribution statement

416 All authors contributed equally to the paper.

417 **Conflicts of interest**

418 The authors declare no conflicts of interest.

419 **References**

- 420 Andrews, D.F. and Herzberg, A.M. (1985). Data: a collection of problems from many fields for the
421 student and research worker. Springer, New York.
- 422 Aarset M. V. (1987). How to identify a bathtub hazard rate. IEEE Transactions on Reliability,
423 36(1), 106-108.
- 424 Dombi, J., Jónás, T. and Tóth, Z.E. (2018). The Epsilon Probability Distribution and its Applica-
425 tion in Reliability Theory, Acta Polytechnica Hungarica, Vol. 15, No.1, pp 197 - 216.
- 426 Dombi, J., Jónás, T., Tóth, Z.E. and Árva, G. (2019). The omega probability distribution and its
427 applications in reliability theory. Qual Reliab Eng Int., 35, 2, 600-626.
- 428 Dombi, J. and Jónás, T. (2020) On an alternative to four notable distribution functions with
429 applications in engineering and the business sciences. Acta Polytech. Hung, 17, 231-252.
- 430 Dombi, J. and Jónás, T. (2021). Advances in the theory of probabilistic and fuzzy data
431 scientific methods with applications. In Studies in Computational Intelligence; Springer:
432 Berlin/Heidelberg, Germany, 814, 1-186.
- 433 Ghitany, M.E., Atieh, B. and Nadarajah, S. (2008). Lindley distribution and its Applications,
434 Mathematical Computation and Simulation, 78, 4, 493-506.
- 435 Haktanir, T., Bajabaa, S. and Masoud, M. (2013). Stochastic analyses of maximum daily rainfall
436 series recorded at two stations across the Mediterranean Sea. *Arabian Journal of Geosciences*, 6:
437 3943-3958. DOI: <https://doi.org/10.1007/s12517-012-0652-0>
- 438 Hussain, T., Bakouch, H.S. and Chesneau, C. (2019). A new probability model with applica-
439 tion to heavy-tailed hydrological data. *Environ Ecol. Stat* 26, 127-151. Available at <https://doi.org/10.1007/s10651-019-00422-7>
- 441 Lindley, D.V. (1958). Fiducial distributions and Bayes theorem, Journal of the Royal Statistical
442 Society, A, 20, 102-107.
- 443 Lindley, D.V. (1965). *Introduction to Probability and Statistics from a Bayesian Viewpoint, Part*
444 *II: inference*, Cambridge University Press, New York.
- 445 Mazucheli, J. and Achcar, J.A. (2011). The Lindley distribution applied to competing risks lifetime
446 data, Computer Methods Programs in Biomedicine, 104, 2, 188-192.
- 447 Murthy, D.N.P., Xie M., and Jiang, R. (2004). Weibull Models, y John Wiley and Sons, Inc.,
448 Hoboken, New Jersey.
- 449 Okorie, I. E. and Nadarajah, S. (2019). On the Omega Probability Distribution. Quality and
450 Reliability Engineering International, 35, 6, 2045-2050.
- 451 Phien, H.N. and Ajirajah, T. J. (1984). Applications of the log Pearson type-3 distribution
452 in hydrology. *Journal of Hydrology*, 73(3-4), 359-372. DOI: [https://doi.org/10.1016/0022-1694\(84\)90008-8](https://doi.org/10.1016/0022-1694(84)90008-8)
- 453 1694(84)90008 - 8.

- 454 Shanker, R. and Mishra, A. (2013). A quasi Lindley distribution , Biometrics & African Journal of
455 Mathematics and Computer Science Research, 6, 4, 64-71.
- 456 Shanker, R., Hagos, F. and Sujatha, S. (2015). On modeling of Lifetimes data using exponential
457 and Lindley distributions, Biometrics & Biostatistics International Journal, 2, 5, 1-9.
- 458 Vuong, Q. H. (1989). Likelihood ratio tests for model selection and non-nested hypotheses. *Econo-*
459 *metrica*, 57(2), 307-333.
- 460 Walpole, R.E., Myers, R.H. and Myers, S.L. (2012). Probability and Statistics for Engineers and
461 Scientists. Pearson Education, Inc, 501 Boylston Street, Suite 900, Boston.
- 462 World Meteorological Organization. (2009). *Guide to Hydrological Practices Volume II Management*
463 *of Water Resources and Application of Hydrological Practices WMO-No. 168 6th*, Chairperson,
464 Publications Board World Meteorological Organization (WMO) 7 bis, avenue de la Paix P.O.
465 Box 2300 CH-1211 Geneva 2, Switzerland.